European Journal of Nuclear Medicine and Molecular Imaging (2023) 51:123–135
https://doi.org/10.1007/s00259-023-06448-1

ORIGINAL ARTICLE

Integrated myocardial flow reserve (iMFR) assessment: diffuse atherosclerosis and microvascular dysfunction are more strongly associated with mortality than focally impaired perfusion

Jonathan B. Moody[1] · Alexis Poitrasson-Rivière[1] · Jennifer M. Renaud[1] · Tomoe Hagio[1] · Mouaz H. Al-Mallah[2] · Richard L. Weinberg[3] · Edward P. Ficaro[1,4] · Venkatesh L. Murthy[4]

Received: 16 July 2023 / Accepted: 17 September 2023 / Published online: 3 October 2023

Abstract

Background and aims Although treatment of ischemia-causing epicardial stenoses may improve symptoms of ischemia, current evidence does not suggest that revascularization improves survival. Conventional myocardial ischemia imaging does not uniquely identify diffuse atherosclerosis, microvascular dysfunction, or nonobstructive epicardial stenoses. We sought to evaluate the prognostic value of *integrated myocardial flow reserve* (iMFR), a novel noninvasive approach to distinguish the perfusion impact of focal atherosclerosis from diffuse coronary disease.

Methods This study analyzed a large single-center registry of consecutive patients clinically referred for rest-stress myocardial perfusion positron emission tomography. Cox proportional hazards modeling was used to assess the association of two previously reported and two novel perfusion measures with mortality risk: global stress myocardial blood flow (MBF); global myocardial flow reserve (MFR); and two metrics derived from iMFR analysis: the extents of focal and diffusely impaired perfusion.

Results In total, 6867 patients were included with a median follow-up of 3.4 years [1st–3rd quartiles, 1.9–5.0] and 1444 deaths (21%). Although all evaluated perfusion measures were independently associated with death, diffusely impaired perfusion extent (hazard ratio 2.65, 95%C.I. [2.37–2.97]) and global MFR (HR 2.29, 95%C.I. [2.08–2.52]) were consistently stronger predictors than stress MBF (HR 1.62, 95%C.I. [1.46–1.79]). Focally impaired perfusion extent (HR 1.09, 95%C.I. [1.03–1.16]) was only moderately related to mortality. Diffusely impaired perfusion extent remained a significant independent predictor of death when combined with global MFR ($p < 0.0001$), providing improved risk stratification (overall net reclassification improvement 0.246, 95%C.I. [0.183–0.310]).

Conclusions The extent of diffusely impaired perfusion is a strong independent and additive marker of mortality risk beyond traditional risk factors, standard perfusion imaging, and global MFR, while focally impaired perfusion is only moderately related to mortality.

Keywords Coronary artery disease · Microvascular disease · Cardiac PET · Absolute myocardial blood flow · Myocardial flow reserve

Edward P. Ficaro and Venkatesh L. Murthy equal contribution as co-senior authors.

✉ Jonathan B. Moody
jmoody@inviasolutions.com

[1] INVIA, LLC, Ann Arbor, MI, USA

[2] Houston Methodist DeBakey Heart and Vascular Center, Houston, TX, USA

[3] Division of Cardiology, Feinberg School of Medicine, Northwestern University, Chicago, IL, USA

[4] Division of Cardiovascular Medicine, Department of Internal Medicine, University of Michigan, Ann Arbor, MI, USA

Abbreviations

CAD	Coronary artery disease
CFC	Coronary flow capacity
PET	Positron emission tomography
MBF	Myocardial blood flow
MFR	Myocardial flow reserve
MPI	Myocardial perfusion imaging
BMI	Body mass index
LV	Left ventricle

Introduction

Myocardial perfusion is determined by the net hemodynamic impact of focal flow-limiting epicardial arterial stenoses, diffuse atherosclerosis, and microvascular disease. Ischemic symptoms arise when perfusion is insufficient for myocardial needs. Although treatment of ischemia-causing epicardial stenoses may improve symptoms [1, 2], current evidence does not suggest that revascularization of epicardial stenoses improves survival [3–5], even in the presence of moderate to severe regional myocardial ischemia. Conversely, large pooled studies have demonstrated a consistent link between the presence of ischemia and adverse outcomes [6]. Further, studies of animal models have demonstrated that ischemia may precipitate life-threatening cardiac arrhythmias [7], myocardial systolic and diastolic dysfunction [8], and myocardial fibrosis [9], all of which contribute to adverse cardiac outcomes. However, conventional myocardial ischemia imaging typically only detects moderate to severe focal stenoses but does not uniquely identify diffuse atherosclerosis, microvascular dysfunction, or mild focal epicardial stenoses. Consequently, it remains unclear whether focal ischemia is causal to major adverse cardiac events, or if it is simply correlated with the presence and extent of coronary atherosclerosis and thus with the potential for acute plaque rupture.

We have developed a novel quantitative approach, *integrated myocardial flow reserve* (iMFR), for separating focal impairment of myocardial perfusion, typically due to focal epicardial stenosis, from diffuse impairment of myocardial perfusion, which may result from diffuse atherosclerosis and/or microvascular dysfunction. Our method uses regional data from quantitative rest-stress myocardial perfusion imaging (MPI) using positron emission tomography (PET). Nearly all prior PET studies of quantitative myocardial perfusion focused only on global measures of perfusion [10–15] and did not disambiguate focal and diffuse components. To our knowledge, only two prior studies [16, 17] evaluated the prognostic importance of focally abnormal quantitative measures of perfusion combining MBF and MFR into coronary flow capacity (CFC). However, these studies did not examine or compare measures of focal and diffusely impaired perfusion and thus could not resolve the ischemia-prognosis paradox. In this study, we sought to evaluate the prognostic value of these two distinct components of iMFR (*i.e.,* focally and diffusely impaired myocardial perfusion) in a large clinical registry of 6867 patients and 25,420 person-years of follow-up.

Methods

Study population

All consecutive patients referred for rest-stress PET-CT assessment of myocardial perfusion at the University of Michigan Cardiovascular Center between March 1, 2011, and July 31, 2020, were considered for inclusion in the registry. Exclusion criteria included history of heart transplantation and missing or uninterpretable PET data. For patients who underwent serial PET imaging, only the first evaluable PET exam was included. All data were anonymized, and informed consent was waived under an exemption from the University of Michigan Institutional Review Board.

Positron emission tomography

All patients were instructed to fast for at least 4 h and to refrain from caffeine consumption for 24 h prior to the imaging exam. Patients underwent ^{82}Rb PET-CT imaging in 3D mode on a PET scanner with lutetium oxyorthosilicate (LSO) detectors (Biograph mCT, Siemens Healthineers, Malvern, PA). An initial low-dose CT scan was acquired for attenuation correction. List-mode ECG-gated time-of-flight (TOF) PET data were acquired at rest for 7 min, beginning with intravenous bolus administration of ^{82}Rb (Cardiogen-82, Bracco Diagnostics, Monroe Township, NJ USA; or RubyFill, Jubilant Radiopharma, Montréal, Québec Canada) using either a weight-adjusted (12 MBq/kg, $N = 2473$ (36%) patients) or BMI-adjusted (33.3 MBq/kg/m^2, $N = 4397$ (64%) patients) dosing protocol. Pharmacologic stress was initiated with bolus administration of regadenoson intravenously (0.4 mg); this was followed 60 s later by administration of the same ^{82}Rb dose and a second list-mode ECG-gated TOF PET acquisition of 7 min. Heart rate and systolic and diastolic blood pressure were monitored during PET scans.

Image reconstruction

PET data were corrected for normalization, dead time, attenuation, decay, scattered, and random coincidence events as part of the scanner vendor's image reconstruction software. The relative position of the heart in PET and CT images for attenuation correction was examined and manually corrected, when necessary, before final image reconstruction. Static and 16-frame ECG-gated images were reconstructed from ^{82}Rb PET list-mode data using the vendor's 3D OSEM reconstruction (3 iterations, 21 subsets) with TOF and point-spread function modeling when available; this was followed by smoothing with a 7-mm full-width half-maximum Gaussian filter. Static and gated ^{82}Rb images excluded the first 2 min of list-mode data to allow blood pool clearance of the tracer. Dynamic PET images

were reconstructed (30 frames: 16 × 5 s, 6 × 10 s, 3 × 20 s, 4 × 30 s, 1 × 90 s) using the full list-mode data without post-reconstruction filtering. A subset of static images was also routinely reconstructed with a dual respiratory and cardiac gated option provided by the PET vendor; these static images were prioritized for analysis at the discretion of the reading physician. The matrix size for all images was 128 × 128 × 75, with an in-plane voxel size of 3.2 × 3.2 mm and a slice thickness of 3 mm.

Outcomes assessment

The primary outcome was mortality from all causes. The vital status of each patient was determined by integrating data from death certificates and hospital records. A secondary outcome of mortality from any cardiac cause was also considered in the analysis.

Measures of myocardial perfusion

Patient images were clinically processed using the Corridor4DM software (INVIA Medical Imaging Solutions, Ann Arbor, MI). PET images of the heart were rotated into short-axis orientation, and the myocardium of the left ventricle (LV) was segmented using an automated algorithm [18]. The LV contours were checked for quality and manually adjusted by experienced operators as necessary. Left ventricular ejection fraction (LVEF) was estimated from stress and rest 16-frame gated PET images, as previously described [18], and the change in LVEF from rest to stress was computed (LVEF reserve).

For the present analysis, saved result files from the original clinical reading of PET exams by board-certified nuclear cardiologists were batch processed in a blinded fashion without user interaction to generate results for all perfusion measures described below. This allowed uniform application of automated dynamic motion correction [19] and consistent kinetic model settings.

Relative myocardial perfusion

Conventional semi-quantitative myocardial perfusion was assessed in each patient. Static PET images were normalized to peak tracer uptake in the LV myocardium, and perfusion polar maps of myocardial uptake were generated [18]. Each pixel of the perfusion polar map was compared to matched ^{82}Rb normal databases derived from low-likelihood patients in order to automatically quantify regional perfusion defect severity in terms of the number of standard deviations below the normal database regional mean. Total perfusion deficit (TPD) at rest and during hyperemia was estimated as a summary measure of defect severity and extent, and ischemic TPD was computed as hyperemic minus rest TPD [20].

Myocardial blood flow (MBF) and flow reserve

Myocardial blood flow was estimated by fitting a 1-tissue-compartment kinetic model to myocardial time activity curves sampled from dynamic PET images, as previously described [21, 22]. The arterial input function was determined from the regional mean of a three-dimensional region of interest automatically placed near the mitral valve plane in each frame of the dynamic image series. Myocardial flow reserve (MFR) was calculated as the ratio of hyperemic to rest MBF. Global stress MBF and MFR were averaged over the whole left ventricle for subsequent assessment, individually and in combination, as predictors of outcome [10].

Integrated myocardial flow reserve (iMFR)

A novel quantitative perfusion analysis was developed to integrate regional MFR and MPI (Fig. 1). A perfusion defect blackout map was created using the relative stress perfusion polar map with a defect severity threshold of 2.5 standard deviations below the normal database regional mean, categorizing each pixel as being within (black) or outside focal perfusion defects. Each pixel was then further categorized by MFR using a threshold of 2.0 [11, 12], yielding up to four LV regions: (1) *normal* perfusion (MFR ≥ 2.0 outside focal defects); (2) *diffusely impaired* perfusion (MFR < 2.0 outside focal defects); (3) *focally impaired* perfusion (MFR < 2.0 within defects); and (4) *focally preserved* perfusion (MFR ≥ 2.0 within defects). The extent of each region was computed as the fraction of LV myocardial pixels, and the diffusely and focally impaired perfusion extents (regions 2 and 3) were evaluated as predictors of outcome.

Statistical analysis

The four perfusion measures, global stress MBF, global MFR, and extents of diffusely and focally impaired MFR (iMFR regions 2 and 3), were individually evaluated as both continuous and categorical variables to assess their association with risk of outcomes. For each continuous measure, two Cox proportional hazards models were constructed, unadjusted and adjusted for clinical risk factors and standard MPI findings. Baseline covariates were selected on the basis of clinical judgment and prior work [10, 11] and included patient age, sex, body mass index (BMI), race, diabetes, hypertension, hyperlipidemia, smoking status, history of myocardial infarction (MI), previous percutaneous coronary intervention (PCI), previous coronary artery bypass graft (CABG), family history of coronary artery disease

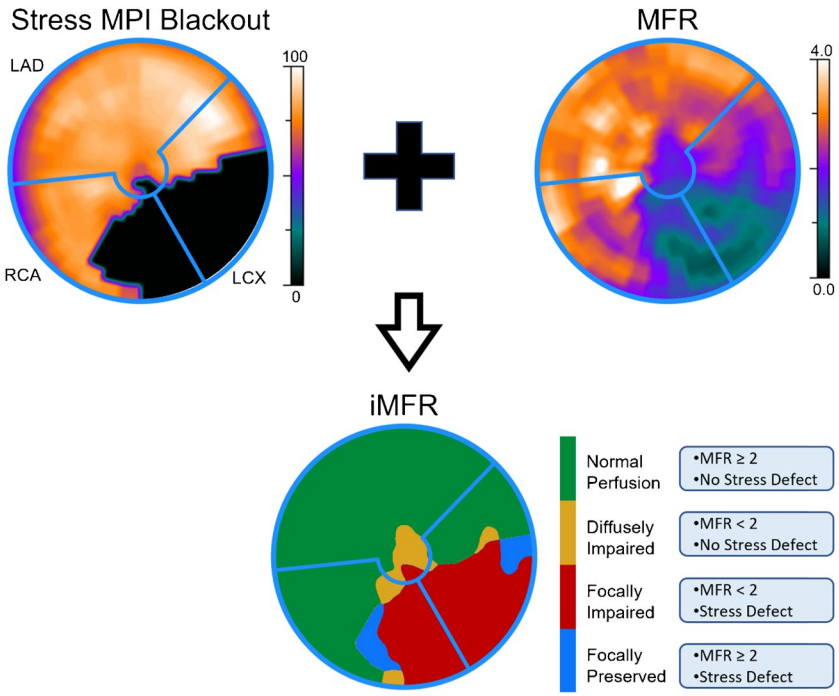

Fig. 1 Example of integrated myocardial flow reserve (iMFR) polar map creation from stress myocardial perfusion imaging (MPI) perfusion blackout and MFR maps. Four iMFR regions are defined in terms of the presence or absence of a regional stress perfusion defect and normal or abnormal MFR (lower right)

(CAD), LVEF at rest, difference between stress and rest LVEF, and stress total perfusion deficit (TPD) as a combined relative measure of ischemia or scar. Nonlinear effects were evaluated using ANOVA tests of models with continuous variables modeled as restricted cubic splines with 3 knots [23], which were found to be necessary for stress MBF and MFR, but not necessary for diffusely or focally impaired perfusion extent. Time to revascularization was modeled as a time-dependent covariate for patients that underwent revascularization after the PET scan. The hazard ratio for each perfusion measure was standardized to 1 × interquartile range (IQR) in the direction of increasing impairment. A secondary analysis was also performed to evaluate standard adjustment for the product of heart rate and systolic blood pressure during the rest PET scan (rate-pressure product, RPP) by multiplying rest MBF by the ratio of a reference RPP (9000 mm Hg bpm) to rest RPP in models with global MFR [24].

For each perfusion measure treated as a categorical variable, patients were assigned to groups based on quintiles of the perfusion measures, except for focally impaired extent. In this case, the lowest category (focally impaired extent equal to zero) contained 48% of patients and the remaining patients were assigned to quartiles. Annualized event rates were evaluated among the quintiles of each perfusion measure using Poisson modeling. Cox proportional hazards models were constructed as described above to evaluate the risk of outcomes with reference to the most normal group (lowest quintile), and unadjusted and adjusted survival curves were computed for each group.

Proportional hazards for Cox models were verified with scaled Schoenfeld residuals. Model calibration was assessed using bootstrap resampling validation of calibration slope. Model discrimination was assessed using model likelihood ratio χ^2 and Gönen and Heller's concordance measure, *K*, which, unlike Harrell's c-index, is insensitive to the rate of censoring [25, 26]. The change in discrimination after adding the extent of diffusely impaired perfusion to individual Cox models of the other perfusion measures was assessed with continuous net reclassification improvement [27]. Sensitivity analyses included additional multivariable Cox models to evaluate: (1) replacing the time-dependent revascularization with a binary variable indicating early revascularization (within 90 days after the PET scan) and (2) including an additional covariate for the time interval from the beginning of the study period (March 1, 2011) to each PET exam, and then testing its interaction with each perfusion measure to account for potential variations in patient referral, reporting, PET dosing protocol, and software during the study period.

Continuous variables are summarized as mean ± SD or median [1st–3rd quartiles]. Welch's unequal variances t-test or Wilcoxon rank sum tests were used as appropriate for comparisons of continuous parameters, and chi-squared tests were used to compare categorical variables. Two-sided *p*-values less than 0.05 were considered statistically significant. Statistical analyses were performed using R version 4.1 [28] with packages *survival* [29], *rms* [23], and *survminer* [30].

Results

Patient characteristics

Out of 7227 unique patients referred for rest-stress PET during the study period, we excluded those evaluated for cardiac allograft vasculopathy ($N=333$, 4.6%), those with missing or uninterpretable dynamic PET images ($N=25$, 0.35%), and those with missing clinical covariates (LVEF) ($N=2$, 0.03%). After these exclusions, a total of 6867 patients remained in the study cohort. Overall mean patient age was 63 ± 12 years, and 3043 (44%) were women. Known CAD (history of MI or previous revascularization) was present in 2114 (31%), and 425 (6%) underwent subsequent revascularization within 90 days after the PET exam. The median follow-up time was 3.4 [1.9–5.0] years. Patient characteristics at baseline stratified by the extent of diffusely impaired MFR (iMFR region 2) are shown in Table 1 and stratified by mortality in Supplementary Table S1. The incidence of hypertension, diabetes, and hyperlipidemia increased with increasing extent of diffusely impaired MFR (Table 1).

Measures of myocardial perfusion

The median global MFR was 2.03 [1.57–2.55], and global stress MBF was 2.06 [1.56–2.64] ml/min/g. Among patients with diffusely impaired perfusion extent > 0, the median extent was 42% [13–76%], and likewise, the median extent of focally impaired perfusion was 9% [2–25%].

Myocardial perfusion and outcomes

All quantitative perfusion measures were significantly associated with the risk of death and cardiac death in individual Cox models (Table 2, model 1). However, after adjusting for demographic covariates, clinical risk factors, and standard MPI findings, both global MFR and diffusely impaired perfusion extent were consistently stronger predictors of primary and secondary outcomes, and the corresponding Cox models had consistently higher χ^2 and concordance K than those of global stress MBF and focally impaired perfusion extent (Table 2, model 2) (Fig. 2). Similar results were seen when comparing the highest versus lowest quintiles (Supplementary Table S3). The association of focally impaired perfusion extent (iMFR region 3) with risk of outcomes was substantially weaker than the other three perfusion measures, which has important physiologic and clinical implications. An interaction between diffusely impaired perfusion extent and transient ischemic dilation was marginally significant ($p=0.034$) with minimal effect size (HR 0.98). Models are summarized in Supplementary Figs. S1–S12. Secondary analyses evaluating the adjustment of rest MBF for the rate-pressure product yielded inferior risk models with MFR (Supplementary Results and Figs. S13 and S14). Sensitivity analyses yielded results largely similar to the primary analysis (Supplemental Results and Figs. S15–S18).

In Cox models evaluating combinations of perfusion measures, diffusely impaired perfusion extent remained a significant independent predictor of all-cause and cardiac death when combined with global MFR ($p<0.0001$ and $p=0.0311$, respectively), or with global stress MBF ($p<0.0001$ for both outcomes) (Table 3). Diffusely impaired perfusion extent was also a significant additive predictor when combined with focally impaired perfusion extent ($p<0.0001$). Conversely, focally impaired perfusion extent did not add significant prognostic value in combination with global MFR or stress MBF. Global stress MBF was not significantly associated with outcomes when combined with global MFR (Supplementary Table S3). Significant increases in overall net reclassification improvement between 0.25 and 0.48 were observed when combining the extent of diffusely impaired perfusion with each of the other perfusion measures (Table 4).

The annualized rate of all-cause death across quintiles of each myocardial perfusion measure increased steadily with increasing degree of impairment (Fig. 3, Supplementary Fig. S19). Similarly, incidence plots demonstrated that successive quintiles of each myocardial perfusion measure were associated with worse prognosis, both before and after adjusting for demographic covariates, clinical risk factors, and standard MPI findings (Supplementary Figs. S11 and S12). Among patients without any diffusely impaired MFR ($N=437$), the annualized rates of all-cause and cardiac death were 1.1% and 0.25%, respectively.

Predicted risk of all-cause mortality as a function of global MFR and diffusely impaired perfusion extent (Table 3, model 1) is shown in Fig. 4, indicating that at any given global MFR less than 2.5, an increase in diffusely impaired perfusion extent was associated with progressively increased risk of mortality. Two case examples are shown in Fig. 5.

Discussion

In this large single-center registry of consecutive patients undergoing comprehensive myocardial perfusion assessment, we have demonstrated that the impact of diffuse atherosclerosis and microvascular dysfunction, as quantified by integrated myocardial flow reserve (iMFR) analysis, is a powerful predictor of mortality, independent of risk factors and relative MPI assessment of hemodynamically obstructive disease and systolic LV function. The association of diffusely impaired perfusion extent with diffuse nonobstructive atherosclerosis and/

Table 1 Patient characteristics at baseline stratified by extent of diffusely impaired MFR

	Extent of diffusely impaired MFR				
	None ($n=437$)	1–42% ($n=3212$)	43–100% ($n=3218$)	Total ($n=6867$)	p-value
Demographics, *N* (%)					
Age (years) †	55 (11)	61 (12)	66 (12)	63 (12)	< 0.001
Male sex	241 (55)	1795 (56)	1788 (56)	3824 (56)	0.941
Race, *N* (%)					
White	329 (75)	2601 (81)	2631 (82)	5561 (81)	0.008
Black	73 (17)	417 (13)	372 (12)	862 (13)	
Other	35 (8)	194 (6)	215 (7)	444 (6)	
Cardiovascular risk factors, *N* (%)					
Hypertension	281 (64)	2346 (73)	2579 (80)	5206 (76)	< 0.001
Diabetes	100 (23)	1031 (32)	1581 (49)	2712 (39)	< 0.001
Hyperlipidemia	262 (60)	2060 (64)	2161 (67)	4483 (65)	0.002
BMI (kg/m^2) †	31.6 (8)	33.5 (9.1)	33.5 (9.7)	33.4 (9.3)	< 0.001
Family history of CAD	271 (62)	2112 (66)	2126 (66)	4509 (66)	0.244
Current smoker	80 (18)	315 (10)	235 (7)	630 (9)	< 0.001
History of MI	53 (12)	586 (18)	599 (19)	1238 (18)	0.004
Prior PCI	57 (13)	651 (20)	598 (19)	1306 (19)	0.001
Prior CABG	14 (3)	302 (9)	378 (12)	694 (10)	< 0.001
Symptoms, *N* (%)					
Angina	278 (64)	1640 (51)	1236 (38)	3154 (46)	< 0.001
Dyspnea	69 (16)	557 (17)	512 (16)	1138 (17)	0.274
Medications, *N* (%)					
Antiplatelet	204 (47)	1550 (48)	1629 (51)	3383 (49)	0.089
ACE inhibitor	86 (20)	767 (24)	872 (27)	1725 (25)	< 0.001
Beta blocker	137 (31)	1272 (40)	1664 (52)	3073 (45)	< 0.001
Insulin	47 (11)	570 (18)	1166 (36)	1783 (26)	< 0.001
Diuretic	95 (22)	1006 (31)	1475 (46)	2576 (38)	< 0.001
Statin	134 (31)	1199 (37)	1470 (46)	2803 (41)	< 0.001
Hemodynamics †					
Rest					
Heart rate (bpm)	69 (12)	71 (13)	76 (14)	73 (14)	< 0.001
Systolic BP (mm Hg)	127 (20)	131 (23)	136 (25)	133 (24)	< 0.001
Diastolic BP (mm Hg)	75 (15)	75 (31)	71 (19)	73 (25)	< 0.001
RPP (mm Hg × bpm)	8698 (1990)	9286 (2360)	10,387 (2624)	9765 (2539)	< 0.001
Stress					
Heart rate (bpm)	99 (18)	93 (18)	91 (25)	92 (22)	< 0.001
Systolic BP (mm Hg)	117 (28)	118 (31)	118 (33)	118 (32)	0.824
Diastolic BP (mm Hg)	68 (36)	66 (33)	61 (38)	64 (36)	< 0.001
PET measurements †					
Rest					
LVEF (%)	60 (12)	56 (16)	56 (16)	56 (15)	< 0.001
TPD (%)	4 (6)	6 (10)	5 (7)	5 (9)	< 0.001
Global MBF (ml/min/g)	0.85 (0.24)	0.96 (0.32)	1.22 (0.43)	1.08 (0.40)	< 0.001
Stress					
LVEF (%)	66 (13)	60 (17)	59 (16)	60 (16)	< 0.001
TPD (%)	4 (7)	8 (13)	7 (9)	7 (11)	< 0.001
Global MBF (ml/min/g)	2.98 (0.83)	2.32 (0.82)	1.87 (0.73)	2.15 (0.84)	< 0.001
LVEF reserve (%)	6 (4)	4 (4)	2 (4)	3 (4)	< 0.001
Ischemic TPD (%)	2 (4)	4 (6)	4 (5)	4 (6)	< 0.001

Table 1 (continued)

	Extent of diffusely impaired MFR				
	None ($n=437$)	1–42% ($n=3212$)	43–100% ($n=3218$)	Total ($n=6867$)	p-value
Global MFR	3.59 (0.58)	2.48 (0.56)	1.56 (0.33)	2.12 (0.75)	< 0.001
Diffusely impaired MFR ‡	–	1.78 (0.16)	1.48 (0.23)	1.53 (0.46)	< 0.001
Focally impaired MFR extent (%)	0.5 (3.7)	7.7 (15.8)	9.5 (13.6)	8.1 (14.4)	< 0.001
Outcomes, *N* (%)					
All-cause mortality	21 (5)	437 (14)	986 (31)	1444 (21)	< 0.001
Cardiac-related mortality	5 (1)	149 (5)	278 (9)	432 (6)	< 0.001

†Mean (SD)

‡Mean MFR within the diffusely impaired region (iMFR region 2)

BMI, body mass index; *BP*, blood pressure; *CABG*, coronary artery bypass graft; *CAD*, coronary artery disease; *LVEF*, left ventricular ejection fraction; *MBF*, myocardial blood flow; *MFR*, myocardial flow reserve; *MI*, myocardial infarction; *PCI*, percutaneous coronary intervention; *RPP*, rate-pressure product; *TPD*, total perfusion deficit

Table 2 Individual models of myocardial perfusion measures as continuous variables and risk of outcomes*

Outcome	Model 1 (unadjusted)		Model 2 (fully adjusted) †			
Perfusion measure	HR (95% C.I.)	p value	HR (95% C.I.)	p value	χ^2 (d.f.)	K § (95% C.I.)
All-cause mortality						
Focally impaired perfusion extent (%)	1.24 (1.21–1.27)	< 0.0001	1.09 (1.03–1.16)	0.0034	774.2 (18)	0.679 (0.668–0.689)
Global stress MBF (ml/min/g)	2.23 (2.07–2.39)	< 0.0001	1.62 (1.46–1.79)	< 0.0001	853.3 (19)	0.687 (0.677–0.698)
Global MFR	2.73 (2.51–2.96)	< 0.0001	2.29 (2.08–2.52)	< 0.0001	1067.6 (19)	0.709 (0.699–0.720)
Diffusely impaired perfusion extent (%)	2.82 (2.55–3.12)	< 0.0001	2.65 (2.37–2.97)	< 0.0001	1063.9 (18)	0.714 (0.704–0.724)
Cardiac-related mortality						
Focally impaired perfusion extent (%)	1.41 (1.35–1.46)	< 0.0001	1.12 (1.02–1.24)	0.0232	546.4 (18)	0.733 (0.719–0.747)
Global stress MBF (ml/min/g)	3.20 (2.76–3.71)	< 0.0001	1.61 (1.33–1.94)	< 0.0001	568.8 (19)	0.739 (0.724–0.755)
Global MFR	3.03 (2.64–3.49)	< 0.0001	1.99 (1.68–2.36)	< 0.0001	611.4 (19)	0.743 (0.729–0.758)
Diffusely impaired perfusion extent (%)	2.31 (1.93–2.77)	< 0.0001	2.26 (1.82–2.81)	< 0.0001	596.8 (18)	0.758 (0.743–0.772)

*Hazard ratios were standardized to 1 × IQR in the direction of increasing impairment

†Model 2 was adjusted for age, sex, BMI, race, hypertension, diabetes, hyperlipidemia, current smoking, history of MI, previous PCI, previous CABG, revascularization after PET, family history of CAD, LVEF at rest, LVEF reserve, and stress TPD

§Concordance probability K is a measure of a model's discriminative power and ranges between 0.5 (no discrimination) and 1 (perfect discrimination) [25]

HR, hazard ratio; *MBF*, myocardial blood flow; *MFR*, myocardial flow reserve

or microvascular dysfunction is consistent with prior studies [31, 32] and our own data in a large clinical cohort ($N=1044$) with invasive angiography correlation [33]. Conversely, focally impaired perfusion extent, also derived from iMFR analysis, may be a powerful predictor of focal atherosclerotic lesions on angiography. However, in this study, focally impaired perfusion extent was only minimally related to survival and was not a significant additive predictor of mortality when combined with other perfusion measures. This combination is in accord with previous findings that the risk of serious adverse events in CAD typically arises from mild to moderate stenoses, which traditionally have not been considered to cause focal abnormalities in myocardial perfusion [34, 35]. Microvascular dysfunction may further augment the risk of death [36, 37], although the exact mechanisms for this are unclear. Our data presented in this work align with prior randomized studies indicating revascularization of focal atherosclerotic lesions does not generally modify prognosis [3–5, 38, 39].

The extent of diffusely impaired myocardium reflects the quantitative mismatch between regionally reduced MFR and apparently normal relative MPI. Diffusely impaired myocardium is defined as being free of relative stress perfusion defects while having regionally impaired MFR < 2.0 [11, 12]. Similarly, focally impaired and focally preserved myocardium are defined by the presence of relative perfusion defects with either regionally impaired or preserved

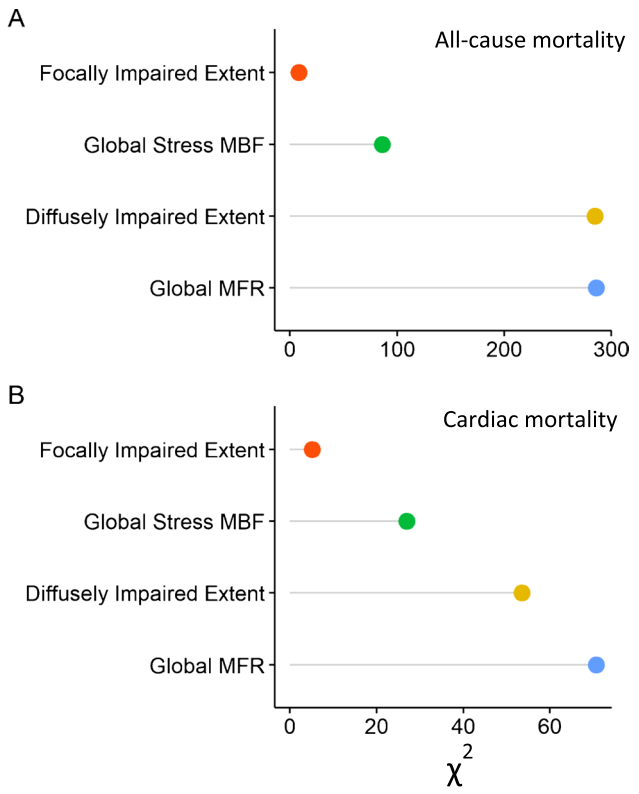

Fig. 2 Variable importance as measured by Wald χ^2 for individual models of myocardial perfusion measures. (**A**) Models of all-cause mortality risk; (**B**) models of cardiac mortality risk. All models were fully adjusted, as in model 2 of Table 2. The χ^2 values represent the increase in model likelihood contributed by each perfusion measure to the base model of demographic covariates, clinical risk factors, and standard MPI findings

MFR. Among these three measures, the extent of diffusely impaired perfusion was the most predictive of the risk of outcomes. Diffusely impaired myocardium was identified in 94% of patients in this study and likely represents a spectrum of diffuse nonobstructive epicardial disease of low to intermediate severity and/or microvascular dysfunction. Importantly, patients without any diffusely impaired myocardium had a very low annualized rate of cardiac mortality (0.25%).

In secondary analyses, we observed that the adjustment of rest MBF for rate-pressure product [24] reduced the association of global MFR with risk of outcomes. This is consistent with previous studies [11] and suggests that such variations in myocardial workload may carry important prognostic information.

Several prior studies have demonstrated that quantitative measures of global myocardial perfusion with PET and cardiac magnetic resonance imaging are associated with prognosis [10–15, 40, 41]. We also found that these metrics carry prognostic value. Prognostic association was consistently stronger and model concordance consistently higher for global MFR and diffusely impaired extent than for global stress MBF and focally impaired extent (Table 2). This finding accords with previous PET findings that global MFR is a stronger predictor of mortality risk than global stress MBF [10, 11]. Importantly, diffusely impaired perfusion extent adds prognostically to global MFR and significantly improves risk stratification, as shown by a significant increase in both event and non-event net reclassification improvement (Table 4). Prior studies that investigated global metrics have not been able to combine metrics for additive prognostic value [10]. Global perfusion measures, which are averaged over the entire LV, inherently blend the effects of focal reductions in flow associated with epicardial disease and impairments associated with diffuse atherosclerosis or microvascular dysfunction. While global metrics may be convenient for analyses, they may overlook relevant regional information [17].

Few prior studies have validated prognostic value for regional or segmental measures. In a recent observational study of 314 patients undergoing ^{15}O-water PET analyzed

Table 3 Combined models of perfusion measures as continuous variables and risk of outcomes*

Outcome	Diffusely impaired extent (%)		Global MFR		Global stress MBF (ml/min/g)			
Model	HR (95% C.I.)	*p* value	HR (95% C.I.)	*p* value	HR (95% C.I.)	*p* value	χ^2 (d.f.)	*K* (95% C.I.)
All-cause mortality								
Combined model 1	1.71 (1.41–2.08)	< 0.0001	1.57 (1.34–1.85)	< 0.0001	–	–	1096.9 (20)	0.714 (0.704–0.724)
Combined model 2	2.49 (2.20–2.81)	< 0.0001	–	–	1.18 (1.06–1.32)	0.0015	1075.2 (20)	0.714 (0.704–0.724)
Cardiac-related mortality								
Combined model 1	1.46 (1.03–2.06)	0.0311	1.58 (1.21–2.06)	0.0001	–	–	616.0 (20)	0.750 (0.735–0.765)
Combined model 2	2.04 (1.61–2.58)	< 0.0001	–	–	1.27 (1.04–1.55)	0.0064	604.8 (20)	0.754 (0.739–0.770)

*Results were standardized to 1 × IQR in the direction of increasing impairment. Models were fully adjusted as in model 2 of Table 2

Table 4 Continuous net reclassification improvement (NRI) at the median follow-up time of 3.4 years after adding the extent of diffusely impaired perfusion (iMFR region 2) to fully adjusted Cox models in combination with each of the other perfusion measures

Outcome Perfusion measure	Overall NRI	Event NRI (%)	Non-event NRI (%)
All-cause mortality			
Focally impaired perfusion extent (%)	0.484 (0.423–0.542)	25.2 (19.8–30.5)	23.2 (20.5–25.7)
Global stress MBF (ml/min/g)	0.404 (0.343–0.464)	16.8 (11.3–22.5)	23.5 (20.9–25.9)
Global MFR	0.246 (0.183–0.310)	12.1 (6.2–17.5)	12.5 (10.1–15.0)
Cardiac-related mortality			
Focally impaired perfusion extent (%)	0.397 (0.291–0.497)	23.6 (13.5–33.2)	16.2 (13.9–18.7)
Global stress MBF (ml/min/g)	0.290 (0.193–0.393)	12.4 (3.0–22.5)	16.6 (14.2–19.0)
Global MFR	0.263 (0.162–0.367)	11.5 (2.1–21.7)	14.8 (12.6–17.2)

Models were fully adjusted as in model 2 of Table 2; 95% confidence intervals are provided in parentheses. Event NRI is the net percentage of patients with an event who were correctly assigned a higher predicted risk after adding diffusely impaired extent (range − 100 to 100). Non-event NRI is the net percentage of patients without an event who were correctly assigned a lower predicted risk after adding diffusely impaired extent. Overall NRI is sum of event and non-event NRI (range − 2 to 2)

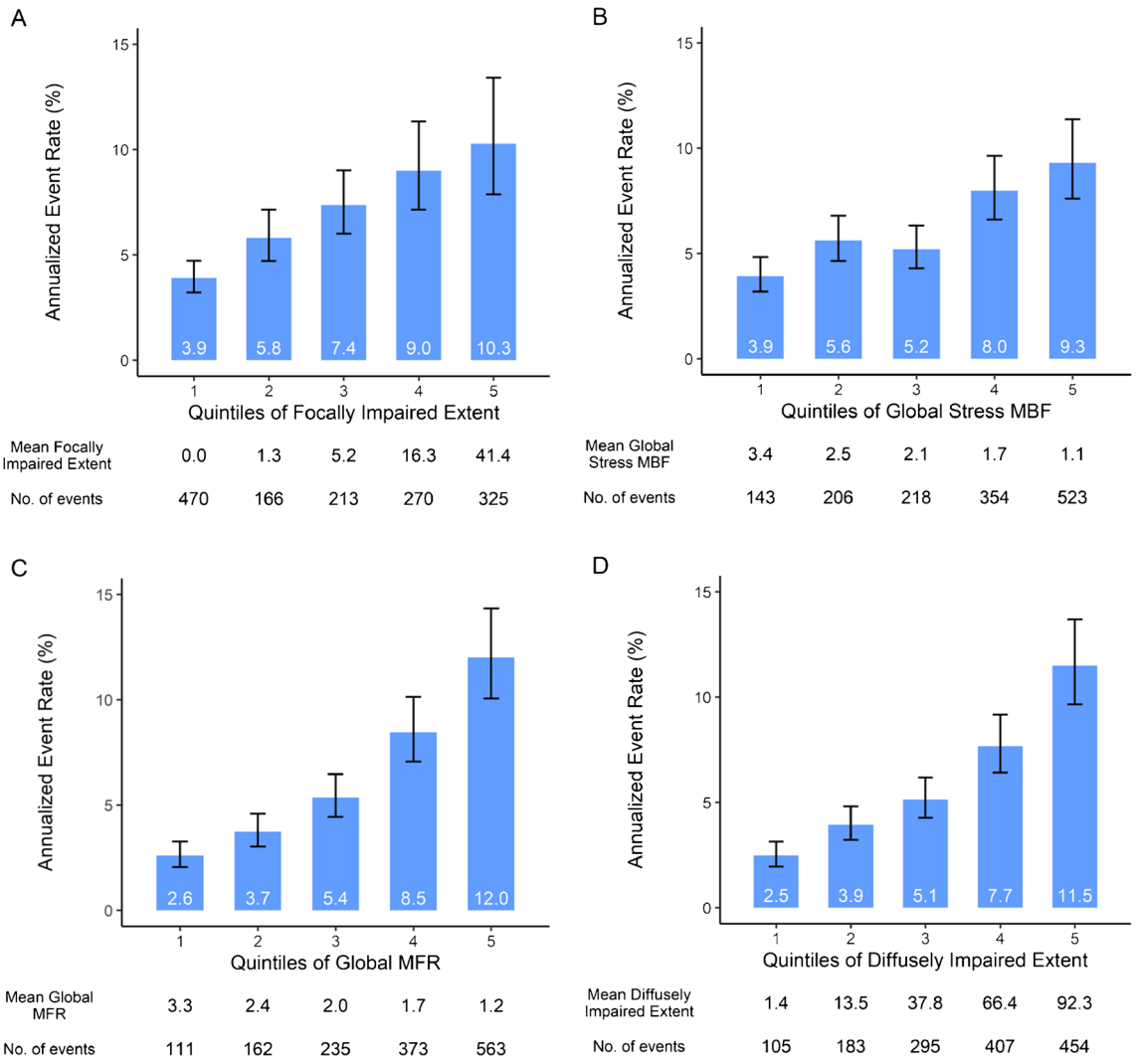

Fig. 3 Adjusted annualized event rates and 95% confidence intervals for all-cause mortality across quintiles of each myocardial perfusion measure. (**A**) Focally impaired perfusion extent (%), (**B**) global stress MBF (ml/min/g), (**C**) global MFR, and (**D**) diffusely impaired perfusion extent (%). For focally impaired extent (**A**), the lowest subgroup (mean extent = 0) contained 3317 patients, and the remaining 3550 patients were divided into quartiles. Individual Poisson models of each perfusion measure were fully adjusted as in model 2 of Table 2

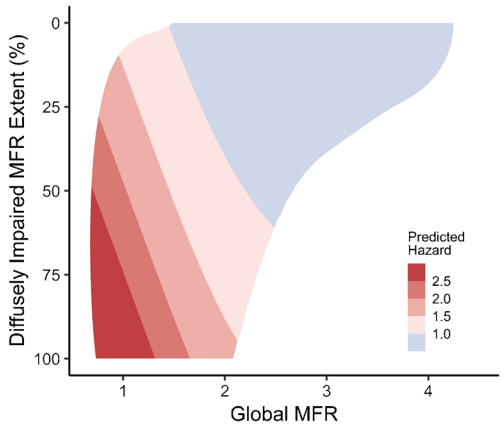

Fig. 4 Predicted risk of all-cause mortality from an adjusted Cox proportional hazards model (Table 3, combined model 1) combining the extent of diffusely impaired MFR (iMFR region 2) and global MFR. The results were fully adjusted as in model 2 of Table 2

using a CFC-like approach, increased CFC at the vascular level was associated with reduced risk of death or non-fatal MI after revascularization [42]. Two other large PET studies ($N = 3774$ and 4995 patients) have demonstrated that the presence of severely impaired CFC is associated with prognosis [16, 17]. CFC analysis combines both stress MBF and MFR into an integrated measure of regional LV perfusion abnormality which quantifies the extent of six CFC categories and scar, each of which combines the severity and extent of regional abnormality [43]. These studies have only demonstrated independent prognostic value for the most impaired CFC category (severely reduced CFC extent), leaving unanswered questions as to the clinical implications of the remaining six categories (including scar).

The iMFR analysis approach differs in several important respects from CFC analysis. By using MFR and not stress MBF, iMFR is expected to be more robust against technical

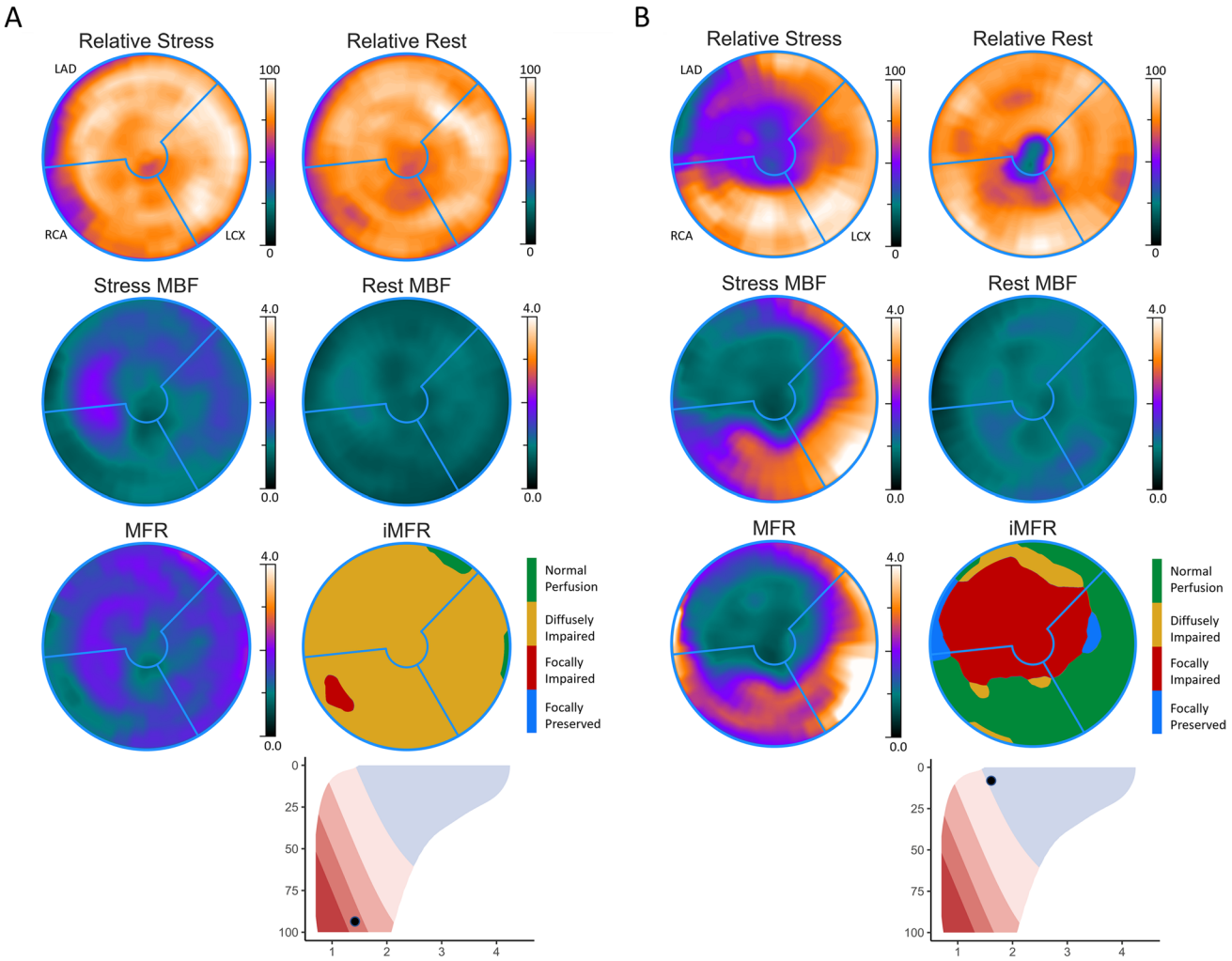

Fig. 5 Case examples with polar maps of PET-derived myocardial perfusion measures. (**A**) Male, 66 years old, global MFR 1.49 and diffusely impaired MFR extent 97%, experienced cardiac-related death 2.7 years after PET exam. (**B**) Male, 64 years old, global MFR 1.77 and diffusely impaired MFR extent 7%, still surviving after 8 years follow-up. The bottom right indicates the predicted risk of all-cause mortality for each patient (black dot), as shown in Fig. 4

and methodologic sources of variability, such as differences in radiotracer characteristics, kinetic modeling approaches, and potential PET scanner saturation [44–47]. iMFR analysis integrates regional MFR with conventional relative MPI processing and relies on a single nominal MFR threshold of 2.0 to yield four possible categories of perfusion impairment. By focusing on quantitative perfusion abnormalities beyond discrete hemodynamically significant defects, the extent of diffusely impaired perfusion identifies the combined effects of nonobstructive coronary disease and/or microvascular dysfunction that are prognostically important.

Limitations

There are a few limitations of our study that should be considered. iMFR was derived from a specific software, and it remains to be demonstrated whether it can be reproducibly obtained using other platforms. Although the thresholds used in iMFR are well validated [11, 12, 48], other combinations of methodologies for each component may generate more discordant results than using single criteria. MFR and perfusion defect data were known to clinicians and thus may have influenced downstream decision-making which in turn may have affected clinical outcomes.

Coronary vasomotor function, as measured by MFR, integrates the effects of microvascular dysfunction with diffuse and focal epicardial CAD. These entities share risk factors and have overlapping pathogenic mechanisms and thus frequently co-exist within the same patient. In this study, we differentiated between focal and diffuse impairments in MFR but did not evaluate epicardial coronary anatomy. The correlation of these findings to epicardial CAD anatomy has been undertaken in a separate study of two large groups of patients [33]. In some individuals, high resting MBF also contributes to diffusely impaired iMFR and is associated with adverse events through mechanisms which may be independent of both epicardial and microvascular disease.

Clinical implications

Conventional myocardial perfusion imaging can detect perfusion abnormalities that are typically associated with moderate-to-severe focal epicardial stenoses but cannot identify diffuse epicardial disease or microvascular dysfunction. Integrated myocardial flow reserve is a novel quantitative approach that extends MPI with the capability to uniquely distinguish focal and diffuse disease components. Our results support a risk assessment approach that considers both global MFR and regional extent of diffusely impaired perfusion. In the presence of abnormal global MFR, an increasing extent of diffusely impaired perfusion confers increasing mortality risk (Fig. 4).

Conclusion

The extent of diffusely impaired perfusion characterizes the burden of diffuse nonobstructive CAD and/or microvascular dysfunction and is a strong independent and additive marker of mortality risk beyond traditional risk factors and standard MPI assessment of hemodynamically obstructive disease and systolic LV function.

Supplementary Information The online version contains supplementary material available at https://doi.org/10.1007/s00259-023-06448-1.

Acknowledgements The authors acknowledge the Regents of the University of Michigan for the use of de-identified clinical data for this study.

Author contribution JBM, APR, JMR, TH, EPF, and VLM contributed to the study conception and design. Material preparation, data collection, and analysis were performed by JBM, APR, JMR, TH, and VLM. The first draft of the manuscript was written by JBM, and all authors reviewed and commented on previous versions of the manuscript. All authors read and approved the final manuscript.

Funding VLM is supported by grants R01AG059729 from the National Institute on Aging, U01DK123013 from the National Institute of Diabetes and Digestive and Kidney Disease, and R01HL136685 from the National Heart, Lung, and Blood Institute as well as the Melvyn Rubenfire Professorship in Preventive Cardiology.

Data availability Individual subject-level data underlying this article cannot be shared publicly due to medical data privacy regulations. The data may be shared on reasonable request under data use agreements with the corresponding author.

Declarations

Ethics approval This is an observational study, and informed consent was waived under an exemption from the University of Michigan Institutional Review Board.

Competing interests JBM, APR, JMR, and TH are employees of INVIA. JMR is a consultant for Jubilant Radiopharma and receives royalties from the licensing of FlowQuant software. EPF is a stockholder in INVIA. MHA has received research support from Siemens Healthineers and is a consultant for Jubilant Radiopharma and Philips Healthcare. RLW has received consulting fees for Ionetix. VLM has received research grants and speaking honoraria from Siemens Healthineers and serves as a scientific advisor for Ionetix and owns stock options in the same. He owns stock in GE and Cardinal Health, has received expert witness payments on behalf of Jubilant DraxImage and a speaking honorarium from 2Quart Medical, and has received payments for consulting from INVIA.

References

1. Spertus JA, Jones PG, Maron DJ, O'Brien SM, Reynolds HR, Rosenberg Y, et al. Health-status outcomes with invasive or conservative care in coronary disease. N Engl J Med. 2020;382(15):1408–19.

2. Al-Lamee RK, Shun-Shin MJ, Howard JP, Nowbar AN, Rajkumar C, Thompson D, et al. Dobutamine stress echocardiography ischemia as a predictor of the placebo-controlled efficacy of percutaneous coronary intervention in stable coronary artery disease. The stress echocardiography–stratified analysis of ORBITA. Circulation. 2019;140(24):1971–80.
3. Boden WE, O'Rourke RA, Teo KK, Hartigan PM, Maron DJ, Kostuk WJ, et al. Optimal medical therapy with or without PCI for stable coronary disease. N Engl J Med. 2007;356(15):1503–16.
4. Maron DJ, Hochman JS, Reynolds HR, Bangalore S, O'Brien SM, Boden WE, et al. Initial invasive or conservative strategy for stable coronary disease. N Engl J Med. 2020;382(15):1395–407.
5. Soares A, Boden WE, Hueb W, Brooks MM, Vlachos HEA, O'Fee K, et al. Death and myocardial infarction following initial revascularization versus optimal medical therapy in chronic coronary syndromes with myocardial ischemia: a systematic review and meta-analysis of contemporary randomized controlled trials. J Am Heart Assoc. 2021;10(2): e019114.
6. Shaw LJ, Iskandrian AE. Prognostic value of gated myocardial perfusion SPECT. J Nucl Cardiol. 2004;11(2):171–85.
7. Janse MJ, Wit AL. Electrophysiological mechanisms of ventricular arrhythmias resulting from myocardial ischemia and infarction. Physiol Rev. 1989;69(4):1049–169.
8. Leone BJ, Norris RM, Safwat A, Foëx P, Ryder WA. Effects of progressive myocardial ischaemia on systolic function, diastolic dysfunction, and load dependent relaxation. Cardiovasc Res. 1992;26(4):422–9.
9. Vilahur G, Juan-Babot O, Peña E, Oñate B, Casaní L, Badimon L. Molecular and cellular mechanisms involved in cardiac remodeling after acute myocardial infarction. J Mol Cell Cardiol. 2011;50(3):522–33.
10. Gupta A, Taqueti VR, van de Hoef TP, Bajaj NS, Bravo PE, Murthy VL, et al. Integrated noninvasive physiological assessment of coronary circulatory function and impact on cardiovascular mortality in patients with stable coronary artery disease. Circulation. 2017;136(24):2325–36.
11. Murthy VL, Naya M, Foster CR, Hainer J, Gaber M, Di Carli G, et al. Improved cardiac risk assessment with noninvasive measures of coronary flow reserve. Circulation. 2011;124(20):2215–24.
12. Ziadi MC, deKemp RA, Williams KA, Guo A, Chow BJW, Renaud JM, et al. Impaired myocardial flow reserve on rubidium-82 positron emission tomography imaging predicts adverse outcomes in patients assessed for myocardial ischemia. J Am Coll Cardiol. 2011;58(7):740–8.
13. Herzog BA, Husmann L, Valenta I, Gaemperli O, Siegrist PT, Tay FM, et al. Long-term prognostic value of ^{13}N-ammonia myocardial perfusion positron emission tomography: added value of coronary flow reserve. J Am Coll Cardiol. 2009;54(2):150–6.
14. Fukushima K, Javadi MS, Higuchi T, Lautamäki R, Merrill J, Nekolla SG, et al. Prediction of short-term cardiovascular events using quantification of global myocardial flow reserve in patients referred for clinical ^{82}Rb PET perfusion imaging. J Nucl Med. 2011;52(5):726–32.
15. Patel KK, Spertus JA, Chan PS, Sperry BW, Al Badarin F, Kennedy KF, et al. Myocardial blood flow reserve assessed by positron emission tomography myocardial perfusion imaging identifies patients with a survival benefit from early revascularization. Eur Heart J. 2020;41(6):759–68.
16. Gould KL, Johnson NP, Roby AE, Nguyen T, Kirkeeide R, Haynie M, et al. Regional, artery-specific thresholds of quantitative myocardial perfusion by PET associated with reduced myocardial infarction and death after revascularization in stable coronary artery disease. J Nucl Med. 2019;60(3):410–7.
17. Gould KL, Kitkungvan D, Johnson NP, Nguyen T, Kirkeeide R, Bui L, et al. Mortality prediction by quantitative PET perfusion expressed as coronary flow capacity with and without revascularization. JACC Cardiovasc Imaging. 2021;14(5):1020–34.
18. Ficaro EP, Lee BC, Kritzman JN, Corbett JR. Corridor4DM: the Michigan method for quantitative nuclear cardiology. J Nucl Cardiol. 2007;14(4):455–65.
19. Lee BC, Moody JB, Poitrasson-Rivière A, Melvin AC, Weinberg RL, Corbett JR, et al. Automated dynamic motion correction using normalized gradient fields for ^{82}rubidium PET myocardial blood flow quantification. J Nucl Cardiol. 2020;28:1982–98.
20. Slomka PJ, Nishina H, Berman DS, Akincioglu C, Abidov A, Friedman JD, et al. Automated quantification of myocardial perfusion SPECT using simplified normal limits. J Nucl Cardiol. 2005;12(1):66–77.
21. Lortie M, Beanlands RSB, Yoshinaga K, Klein R, Dasilva JN, DeKemp RA. Quantification of myocardial blood flow with ^{82}Rb dynamic PET imaging. Eur J Nucl Med Mol Imaging. 2007;34(11):1765–74.
22. Moody JB, Murthy VL, Lee BC, Corbett JR, Ficaro EP. Variance estimation for myocardial blood flow by dynamic PET. IEEE Trans Med Imaging. 2015;34(11):2343–53.
23. Harrell Jr FE (2021) rms: regression modeling strategies. R package version 6.2–0 [Internet]. Available from:https://CRAN.R-project.org/package=rms.
24. Czernin J, Muller P, Chan S, Brunken R, Porenta G, Krivokapich J, et al. Influence of age and hemodynamics on myocardial blood flow and flow reserve. Circulation. 1993;88(1):62–9.
25. Gönen M, Heller G. Concordance probability and discriminatory power in proportional hazards regression. Biometrika. 2005;92(4):965–70.
26. Korn EL, Simon R. Measures of explained variation for survival data. Stat Med. 1990;9(5):487–503.
27. Leening MJG, Vedder MM, Witteman JCM, Pencina MJ, Steyerberg EW. Net Reclassification Improvement: computation, interpretation, and controversies: a literature review and clinician's guide. Ann Intern Med. 2014;160(2):122–31.
28. R Core Team (2021) R: a language and environment for statistical computing [Internet]. Vienna, Austria: R Foundation for Statistical Computing. Available from:http://www.R-project.org/.
29. Therneau TM (2021) A package for survival analysis in R. R package version 3.2–11 [Internet]. Available from:https://CRAN.R-project.org/package=survival.
30. Kassambara A, Kosinski M, Biecek P (2021) survminer: drawing survival curves using "ggplot2". R package version 0.4.9 [Internet]. Available from:https://CRAN.R-project.org/package=survminer.
31. Naya M, Murthy VL, Blankstein R, Sitek A, Hainer J, Foster C, et al. Quantitative relationship between the extent and morphology of coronary atherosclerotic plaque and downstream myocardial perfusion. J Am Coll Cardiol. 2011;58(17):1807–16.
32. Ziadi MC, deKemp RA, Williams K, Guo A, Renaud JM, Chow BJW, et al. Does quantification of myocardial flow reserve using rubidium-82 positron emission tomography facilitate detection of multivessel coronary artery disease? J Nucl Cardiol. 2012;19(4):670–80.
33. Poitrasson-Rivière A, Moody JB, Renaud JM, et al. Integrated myocardial flow reserve (iMFR) assessment: optimized PET blood flow quantification for diagnosis of coronary artery disease. European Journal of Nuclear Medicine and Molecular Imaging 2023;In press.
34. Little WC, Constantinescu M, Applegate RJ, Kutcher MA, Burrows MT, Kahl FR, et al. Can coronary angiography predict the site of a subsequent myocardial infarction in patients with mild-to-moderate coronary artery disease? Circulation. 1988;78(5):1157–66.
35. Erlinge D, Maehara A, Ben-Yehuda O, Bøtker HE, Maeng M, Kjøller-Hansen L, et al. Identification of vulnerable plaques and

patients by intracoronary near-infrared spectroscopy and ultrasound (PROSPECT II): a prospective natural history study. Lancet. 2021;397(10278):985–95.
36. Gdowski MA, Murthy VL, Doering M, Monroy-Gonzalez AG, Slart R, Brown DL. Association of isolated coronary microvascular dysfunction with mortality and major adverse cardiac events: a systematic review and meta-analysis of aggregate data. J Am Heart Assoc. 2020;9(9): e014954.
37. Kelshiker MA, Seligman H, Howard JP, Rahman H, Foley M, Nowbar AN, et al. Coronary flow reserve and cardiovascular outcomes: a systematic review and meta-analysis. Eur Heart J. 2022;43(16):1582–93.
38. The BARI 2D Study Group (2009) A randomized trial of therapies for type 2 diabetes and coronary artery disease. N Engl J Med 360(24):2503–15.
39. McFalls EO, Ward HB, Moritz TE, Goldman S, Krupski WC, Littooy F, et al. Coronary-artery revascularization before elective major vascular surgery. N Engl J Med. 2004;351(27):2795–804.
40. Knott KD, Seraphim A, Augusto JB, Xue H, Chacko L, Aung N, et al. The prognostic significance of quantitative myocardial perfusion. Circulation. 2020;141(16):1282–91.
41. Seraphim A, Dowsing B, Rathod KS, Shiwani H, Patel K, Knott KD, et al. Quantitative myocardial perfusion predicts outcomes in patients with prior surgical revascularization. J Am Coll Cardiol. 2022;79(12):1141–51.
42. de Winter RW, Jukema RA, van Diemen PA, Schumacher SP, Driessen RS, Stuijfzand WJ, et al. The impact of coronary revascularization on vessel-specific coronary flow capacity and long-term outcomes: a serial [^{15}O]H_2O positron emission tomography perfusion imaging study. Eur Heart J - Cardiovasc Imaging. 2022;23(6):743–52.
43. Johnson NP, Gould KL. Integrating noninvasive absolute flow, coronary flow reserve, and ischemic thresholds into a comprehensive map of physiological severity. JACC Cardiovasc Imaging. 2012;5(4):430–40.
44. Murthy VL, Lee BC, Sitek A, Naya M, Moody JB, Polavarapu V, et al. Comparison and prognostic validation of multiple methods of quantification of myocardial blood flow with ^{82}Rb PET. J Nucl Med. 2014;55(12):1952–8.
45. Moody JB, Lee BC, Corbett JR, Ficaro EP, Murthy VL. Precision and accuracy of clinical quantification of myocardial blood flow by dynamic PET: a technical perspective. J Nucl Cardiol. 2015;22(5):935–51.
46. Lee BC, Moody JB, Weinberg RL, Corbett JR, Ficaro EP, Murthy VL. Optimization of temporal sampling for ^{82}rubidium PET myocardial blood flow quantification. J Nucl Cardiol. 2017;24(5):1517–29.
47. Arida-Moody L, Moody JB, Renaud JM, Poitrasson-Rivière A, Hagio T, Smith AM, et al. Effects of two patient-specific dosing protocols on measurement of myocardial blood flow with 3D ^{82}Rb cardiac PET. Eur J Nucl Med Mol Imaging. 2021;12(48):3835–46.
48. Garcia EV, Van Train K, Maddahi J, Prigent F, Friedman J, Areeda J, et al. Quantification of rotational thallium-201 myocardial tomography. J Nucl Med. 1985;26(1):17–26.